

# Advanced MRI of Cartilage and Subchondral Bone in Osteoarthritis

Gregory Chang and Ravinder R. Regatte

**Abstract** Osteoarthritis is a degenerative joint disorder that predominantly affects cartilage and subchondral bone. Magnetic resonance imaging (MRI) provides a noninvasive means to detect pathologic alterations in these two tissues. In this chapter, we provide an overview of MRI techniques to evaluate cartilage and subchondral bone macrostructure, and cartilage biochemical composition [T1rho mapping, T2 mapping,  $^{23}\text{Na}$  MRI, glycosaminoglycan chemical exchange saturation transfer, diffusion tensor imaging (DTI)]. The ability to detect early and short-term changes in the knee joint in vivo will allow new insight into the pathogenesis of osteoarthritis and may permit early diagnosis of osteoarthritis in at-risk subjects. This knowledge and capability should ultimately accelerate the discovery and testing of novel therapies to treat osteoarthritis, a disease which represents an enormous socioeconomic and health burden on society.

## 1 Osteoarthritis Epidemiology

According to the Centers for Disease Control, osteoarthritis (OA) affects 46 million Americans [1]. Joint deformity, pain, and decreased mobility are the main morbidities, resulting in an estimated \$127 billion in annual costs [2]. The risk of disability attributable to knee OA alone is as great as that due to cardiac disease and greater than that due to any other medical condition in elderly persons [2]. Despite great efforts by the pharmaceutical industry and academia, no therapy exists to prevent or

---

G. Chang (✉) • R.R. Regatte  
Quantitative Multinuclear Musculoskeletal Imaging Group (QMMIG), Center for Biomedical Imaging, Department of Radiology, New York University Langone Medical Center, 660 1st Avenue, 4th Floor, New York, NY 10016, USA  
e-mail: [gregory.chang@nyumc.org](mailto:gregory.chang@nyumc.org)

reverse the structural damage of osteoarthritis, and interventions are limited to pain control and, ultimately, joint replacement.

## 2 Pathological Alterations in Cartilage and Subchondral Bone

In the healthy synovial joint, articular cartilage is the primary weight-bearing surface (2–4 mm in thickness) and is composed of an extracellular, fluid-filled matrix of type 2 collagen fibrils and proteoglycans (aggrecan) in which chondrocytes are sparsely distributed [3]. Proteoglycans cross-link collagen fibrils and serve to provide tensile and compressive strength to the matrix [4]. Deep to articular cartilage is a layer of corticalized bone, the subchondral bone plate, which itself is buttressed by subchondral trabecular bone, an intricately connected 3D-network of trabecular plates and rods (50–200  $\mu\text{m}$  in dimension) [5]. The microarchitecture of this trabecular network can be characterized quantitatively in terms of trabecular number, thickness, separation, connectivity, and plate-to-rod ratio, and it is altered in states of high bone turnover or in response to mechanical loading at the joint [6].

Though originally conceptualized as a disorder of articular cartilage, osteoarthritis is now recognized as a disorder involving abnormal mechanical loading at the joint and damage to nearly all articular structures (menisci, synovium, ligaments), but especially articular cartilage and subchondral bone [7, 8]. Degeneration in articular cartilage is initially manifested by loss of proteoglycans and disruption of the type 2 collagen network [3, 9]. This results in loss of tensile and compressive strength of the cartilage matrix, and is followed by morphologic defects such as ulceration of the superficial layer of cartilage and decreased cartilage thickness [3, 9].

In parallel, subchondral bone structure is markedly altered. Beyond the radiographic demonstration of subchondral bone sclerosis, *ex vivo* histomorphometric and high-resolution micro-computed tomography (CT) studies reveal thickening of the subchondral bone plate and remodeling of trabecular bone microarchitecture, including increased trabecular thickness and number, and decreased trabecular separation in OA subjects compared to controls [5, 10–13]. Such trabecular bone micro-architectural alterations are believed to affect the biomechanical competence of bone in ways that cannot be predicted by bone density or bone volume fraction measurements alone [6, 10].

The ability to magnetic resonance imaging (MRI) to noninvasively monitor pathologic alterations in both cartilage and bone in OA subjects *in vivo* (and without the use of ionizing radiation such as in computed tomography studies) provides great insight into the pathogenesis of OA.

**Fig. 1** High-resolution axial 7 T MR image (3-D FLASH, TR/TE = 26/4 ms,  $0.234 \times 0.234 \times 1$  mm) shows up to full thickness cartilage loss (*arrow*) at the median ridge of the patella in a patient with osteoarthritis



### 3 Morphological MRI of Osteoarthritis

#### 3.1 Cartilage

On conventional MRI, numerous sequences exist to evaluate articular cartilage morphology [9]. The most commonly used sequences include fat-suppressed three-dimensional gradient-recalled echo techniques [14, 15] and fast-spin echo techniques without or with fat-suppression [16, 17]. These techniques have reported sensitivities and specificities for the detection of morphologic cartilage defects near or greater than 90 % in the knee when arthroscopy is used as the gold standard for comparison [14, 16].

Fat-suppressed T1-weighted gradient-echo images depict subchondral bone as dark, cartilage as hyperintense, and synovial fluid as lower in signal intensity (Fig. 1). Because a 3-D dataset can be obtained, they are considered ideal for quantitative assessment of cartilage thickness and volume [9]. One drawback is that they are time-consuming (6–15 min) especially when high-resolution images (0.3–0.4 mm in-plane, 1–2 mm slice thickness) are obtained. In addition, gradient-echo images are not ideal for the evaluation of other joint tissues, such as ligaments and menisci.

Fast-spin echo images (Fig. 2) are typically performed with proton density weighting and depict cartilage as intermediate in signal intensity, fluid as hyperintense, and subchondral bone as hyper- or hypointense depending on whether fat-suppression is used. Because fast-spin echo images are 2-D, they are not used for quantitation of cartilage thickness and volume, but they can be used to assess other joint structures, such as ligaments and menisci.

**Fig. 2** Coronal clinical 7 T MR image (fast-spin echo, TR/TE = 1,800/26 ms,  $0.5 \times 0.5 \times 2$  mm) shows marked cartilage loss within the medial compartment (*arrow*) and osteophyte formation (*arrowhead*)



### 3.2 Subchondral Bone

Because conventional MRI sequences only depict subchondral bone as hyperintense or hypointense, the evaluation of subchondral bone is limited to assessment of the size, spatial distribution, and pattern of subchondral bone marrow lesions (BMLs). These BMLs can reflect edema, hemorrhage, vascularity, or fibrosis. BMLs are typically evaluated on fluid-sensitive fat-suppressed sequences. They can be semi-quantitatively assessed according to the whole organ MRI score [18]. Alternatively, it is also possible to quantify the volume of BMLs [19].

BMLs are associated with overlying cartilage defects [20]. Baseline BML volume has been shown to correlate with longitudinal changes in cartilage thickness [21] and predict later cartilage volume loss [22]. Enlarging BMLs are especially associated with cartilage loss [23]. Finally, BMLs in the knee are associated with knee pain [24, 25].

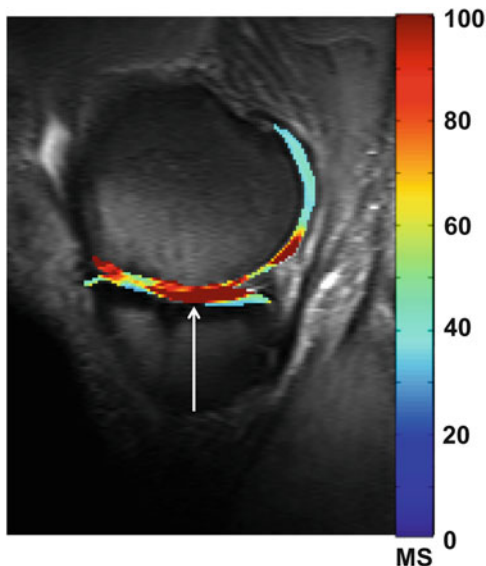
## 4 Advanced MRI of Osteoarthritis

### 4.1 Cartilage

#### 4.1.1 T2 Mapping

Cartilage T2 relaxation value mapping is a potential tool to quantitatively assess cartilage water content and collagen architecture in vivo (Fig. 3) [9, 26–28]. T2 values reflect the dipolar interaction of water protons, which have limited mobility in the highly anisotropic cartilage extracellular matrix. In early cartilage degeneration,

**Fig. 3** Sagittal T2 map of the medial knee compartment shows elevated cartilage T2 values (*arrow*) in a patient with osteoarthritis



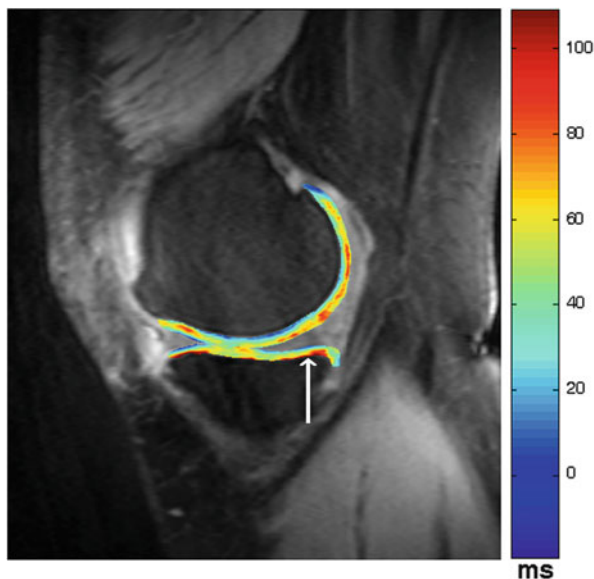
there is evidence for loss of the normal collagen framework [29] and increased water content [30, 31], both of which lead to increased cartilage T2 values [32, 33]. The potential value of T2 mapping as a biomarker for early cartilage degeneration is highlighted by its inclusion in the MRI protocol for the osteoarthritis initiative [34], a nationwide National Institutes of Health-funded observational study that aims to better understand how to prevent and treat osteoarthritis.

The T2 map is generated by: (1) obtaining a series of multiecho spin-echo images, (2) fitting the signal intensity of each pixel to a mono-exponential decay to compute the T2 value for each pixel, and (3) representing each pixel's T2 value with a color scale to create a "map," which is typically overlaid onto the anatomic image of the joint. At 3 Tesla, T2 values of knee cartilage ranges from approximately 30 to 50 ms. There is a well-known spatial variation in cartilage T2 values with higher T2 values closer to the articular surface [26, 35]. In addition, collagen orientation [36] and mechanical loading can also affect T2 values [37, 38], the latter likely through altered water content. Some recent promising studies have provided evidence that elevated knee cartilage T2 values at baseline may predict cartilage morphologic abnormalities at 2 years [39] and 3 years [40].

#### 4.1.2 T1rho Mapping

Cartilage T1rho relaxation value mapping is a potential tool to quantitatively assess cartilage proteoglycan content in vivo (Fig. 4) [41–43]. The T1rho value reflects low frequency spin interactions (100 Hz–10 kHz) and is also known as T1 or spin lattice relaxation in the rotating frame. While cartilage T1 and T2 values are intrinsic

**Fig. 4** Sagittal T1rho map of the medial knee compartment shows spatial variation in cartilage T1rho values (*arrow*) in a patient with osteoarthritis



properties of a tissue, cartilage T1rho values are determined by both the tissue properties and MRI sequence parameters, in particular, the amplitude of the spin-locking pulse.

To perform T1rho mapping, the transverse magnetization is prepared using a long duration, lower power radiofrequency pulse known as the spin-lock pulse. The duration of this pulse is known as the time of spin-lock. It is during the time of spin-lock that the transverse magnetization undergoes relaxation with a rate of  $1/T1\rho$ . Multiple different types of molecular interactions (J-coupling, chemical shift, dipole–dipole, chemical exchange) contribute to the T1rho relaxation [41]. Similar to the T2 map, the T1rho map is generated by representing each pixel's T1rho value using a color look-up table and generation of a color map, which is overlaid onto an anatomic image.

In bovine cartilage specimens, T1rho values change linearly with changes in proteoglycan content [43], but there is also some evidence that collagen content may affect T1rho values as well [44]. In human cartilage specimens with normal T2 values, T1rho values correlate with cartilage proteoglycan content [45]. The high dynamic range of cartilage T1rho values in osteoarthritic human cartilage specimens suggest that it may be well-suited to monitor small changes in cartilage molecular composition and thus disease progression in humans [42]. In humans in vivo, elevated T1rho values correlate with cartilage degeneration [33], and altered T1rho values may serve as a marker for arthroscopically confirmed outerbridge grade 1 and 2 cartilage lesions [46]. Finally, one recent study has provided evidence that elevated knee cartilage T1rho values at baseline may predict cartilage morphologic abnormalities at 2 years [39].

Disadvantages of T1rho mapping include long scan times to acquire images with different spin-lock times and possible issues with specific absorption rate/energy deposition at higher field strength.

### 4.1.3 Delayed Gadolinium Enhanced MRI of Cartilage

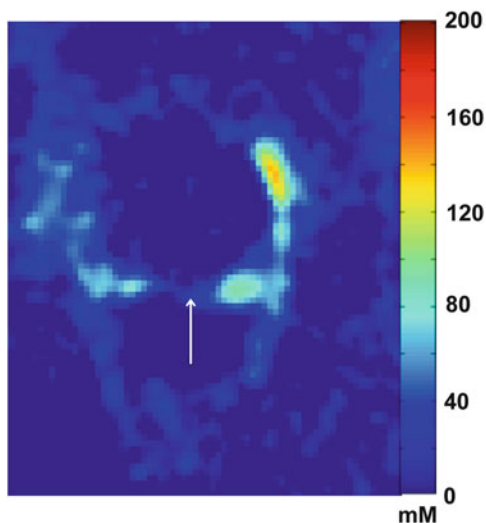
Delayed gadolinium enhanced MRI of cartilage (dGEMRIC) is a method to assess cartilage proteoglycan content. Ions within the interstitial fluid of the cartilage extracellular matrix are distributed in relation to matrix levels of negatively charged glycosaminoglycans. Therefore, after administration of the anionic contrast agent Gd-DTPA<sup>2-</sup>, the degree of penetration of Gd-DTPA<sup>2-</sup> into the cartilage extracellular matrix is inversely related to matrix glycosaminoglycan content [3, 9]. Since Gd has a T1 shortening effect, cartilage T1 relaxation values can be used to estimate Gd concentration and thus cartilage glycosaminoglycan content.

To perform dGEMRIC, the patient is first injected intravenously with a dose of Gd-DTPA<sup>2-</sup> (0.2 mM/kg, twice the recommended clinical dose) and is asked to exercise (e.g., walk on a treadmill) for approximately 10 min. The MRI and T1 mapping is performed 60–90 min after the contrast injection. Together, joint motion and the delay of imaging facilitates the entry of contrast into the joint. The T1 map is computed from a series of images with different T1 weighting. The recent development of a B1 insensitive two-dimensional (D) T1 mapping sequence [47] and a method to correct for B1 inhomogeneity in a 3-D variable flip-angle gradient-echo sequences [48] may allow for more accurate calculation of T1 values. The T1 maps are reported as the dGEMRIC index, with lower values corresponding to lower glycosaminoglycan levels.

In vitro and in vivo studies have shown that dGEMRIC measurements correlate well with reference standard measurements of glycosaminoglycans [49, 50]. In one cross-sectional study of patients with hip dysplasia, the dGEMRIC index correlated significantly with pain and severity of the hip dysplasia and differed significantly between mild, moderate, and severe dysplasia groups [51]. Other studies have provided evidence that a low dGEMRIC index at baseline may predict the development of osteoarthritis on radiographs at 6 years [52] or the later development of joint failure in patients undergoing periacetabular osteotomies [53]. Because of the wide intra- and inter-subject variation in dGEMRIC indices, a standardized dGEMRIC score ( $z$ -score based on number of standard deviations from the mean T1 value in the region of interest) has been proposed to increase the sensitivity for detection of abnormalities [54].

Disadvantages of dGEMRIC include the need for administration of an intravenous contrast agent, which is contraindicated in patients with renal dysfunction due to the increased risk of nephrogenic systemic sclerosis and the long examination time due to the delay after contrast injection.

**Fig. 5** Sagittal sodium concentration map of the medial knee compartment shows markedly decreased cartilage sodium content (*arrow*) in a patient with osteoarthritis



#### 4.1.4 Sodium MRI

Sodium MRI is another method to evaluate cartilage proteoglycan content (Fig. 5). Because of the negative fixed charged density of glycosaminoglycans in the cartilage extracellular matrix, positively charged sodium ions penetrate into the interstitial fluid of the cartilage matrix in relation to the levels of glycosaminoglycans [4, 41]. That is, the lower cartilage glycosaminoglycan content results in lower sodium signal on MR images.

The sodium signal is approximately 4,000 times less than the proton signal [55]. This is because: (1) the sensitivity of MRI for sodium ions is only 9.2 % that of the MR sensitivity for protons and (2) the concentration of sodium ions in vivo is approximately 366 times lower than the water proton concentration. In addition, it should be noted that in intermediate regimes such as biological tissues, the nonspherical sodium nucleus demonstrates a quadrupolar interaction with surrounding electric field gradients. This results in multiple quantum coherences and biexponential T2 relaxation rates, with 60 % of the sodium signal relaxing rapidly (T2 value = 1–2 ms) and 40 % of the sodium signal relaxing more slowly (T2 value = 8–15 ms).

To perform sodium MRI, a dedicated coil tuned to the sodium Larmor frequency is required. Furthermore, because of sodium's rapid transverse relaxation and the already low baseline low signal-to-noise ratio of sodium MRI, imaging is facilitated by the implementation of ultrashort echo time (UTE) sequences and by the performance of imaging at high field (3 Tesla) and ultra high field (7 Tesla).

In trypsin-treated bovine cartilage specimens, cartilage proteoglycan content correlates strongly with sodium signal on MR images [56]. Because of the negative fixed charged density of proteoglycans in cartilage, it is possible to quantify cartilage



sodium concentration [57]. And in vivo, osteoarthritis subjects have demonstrated lower cartilage sodium concentration compared to healthy subjects [4, 58]. The recent development of a fluid-suppressed sodium inversion recovery sequence [59, 60] may improve the quantitation of sodium concentration in cartilage, since synovial fluid also contains sodium and can potentially confound results (Fig. 5).

Disadvantages of sodium MRI include the need for dedicated radiofrequency coils tuned to the sodium Larmor frequency and the lower spatial resolution/longer imaging times that result from low SNR.

#### 4.1.5 Glycosaminoglycan Chemical Exchange Saturation Transfer

Glycosaminoglycan chemical exchange saturation transfer (gagCEST) has been proposed as a method to assess cartilage proteoglycan content [61, 62]. The basis of gagCEST is the detection of the magnetization associated with amide and hydroxyl groups of GAG molecules. Normally, the protons of these groups exchange with water protons. If this exchange is slow, then saturation of the exchange protons of the hydroxyl groups with a long RF pulse leads to attenuation of the water signal in proportion to the concentration of the hydroxyl groups and thus GAG molecules. A two-frequency irradiation approach has been proposed to discriminate CEST effects from magnetization transfer asymmetry effects [63].

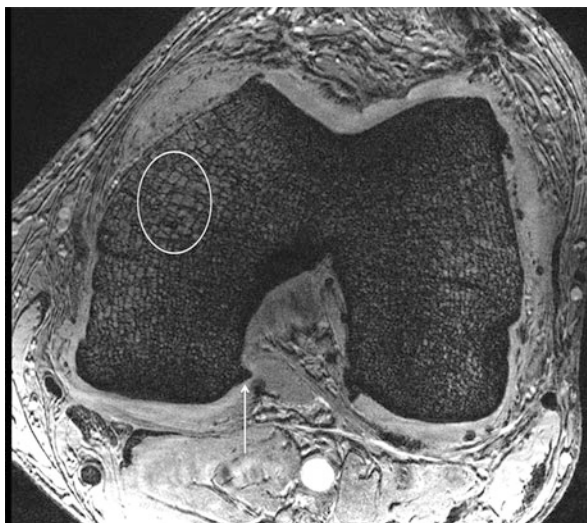
Disadvantages of gagCEST include the need for high field strength, the critical dependence on  $B_0$  field homogeneity, and the possible challenges of isolating gagCEST effects from magnetization transfer effects.

#### 4.1.6 Diffusion Tensor Imaging

Diffusion tensor imaging (DTI) represents a potential means to assess both cartilage proteoglycan and collagen content [64–67]. The rationale behind DTI is that proteoglycan and collagen restrict the motion of water molecules in different manners, which are reflected in diffusion parameters. Proteoglycans do not have anisotropy and restrict the displacement of water molecules in all directions, which can be reflected in the parameter mean diffusivity. Collagen fibers demonstrate anisotropy as they are oriented parallel to the articular surface superficially and perpendicular to subchondral bone in the deep cartilage layer. Water diffusion preferentially occurs along the direction of the collagen fibers, and this can be reflected by the parameter fractional anisotropy.

To perform DTI, multiple magnetic field gradients are applied in several directions to acquire a series of diffusion-weighted images. Each set of images provides information about diffusivity in that direction; their combination produces a map of the diffusion tensor. Eigenvalues and eigenvectors describe the magnitude and directions of the diffusion tensor, which can be represented by an ellipsoid. Mean diffusivity is calculated from the average of the three diffusion tensor eigenvalues.

**Fig. 6** Axial high-resolution 7 T MR image (3-D FLASH, TR/TE = 26/5.1 ms,  $0.234 \times 0.234 \times 1$  mm) of trabecular bone microarchitecture of the knee shows osteophyte formation (*arrow*) and decreased trabecular number and connectivity (*circle*) in the medial femoral condyle of a patient with osteoarthritis



Fractional anisotropy also is calculated from the diffusion tensor eigenvalues, and it reflects the degree of anisotropy within a voxel.

DTI in cartilage demands high SNR. Thus imaging is facilitated by the move to higher field strength. Recently, in a small study involving ten patients with osteoarthritis, Raya et al. [64] showed that ADC and FA calculated from DTI may provide high sensitivity and specificity for the detection of patients with osteoarthritis.

## 4.2 Subchondral Bone

### 4.2.1 MRI of Bone Microarchitecture

The use of advanced MRI techniques combined with digital image analysis methods to quantify bone microarchitecture could provide additional insight into the role of subchondral bone in osteoarthritis pathogenesis. MRI of bone microarchitecture is indirect. The MRI scanner detects magnetization from mobile water and fat protons from within the marrow space and bony trabeculae, which contains solid-state protons that are devoid of signal, are outlined by the hyperintense surrounding marrow.

Because trabeculae are small (100–200  $\mu\text{m}$  thick), MRI of bone microarchitecture requires imaging with high-resolution and voxel sizes that are on the order of the size of the trabeculae (Fig. 6). As a result, high-resolution MRI of bone microarchitecture is a high-SNR demand technique that is facilitated by imaging at higher field strength [68]. Different types of MRI pulse sequences have

been used for imaging bone microarchitecture, including fast large angle spin-echo, steady-state free precession, and gradient-recalled echo techniques [6]. Bone microarchitecture analysis can be performed with digital image analysis methods such as fuzzy distance transform [69], digital topological analysis [70], and finite element analysis [71], which allow quantification of morphologic, topologic, and mechanical properties of bone, respectively.

In the presence of knee malalignment, high-resolution MRI studies reveal elevated bone microarchitectural parameters (bone formation) associated with cartilage loss within the diseased compartment [72]. There is also bone loss within the contralateral compartment [72]. An inverse correlation has also been demonstrated between cartilage T1rho and T2 values and apparent trabecular number, separation, and bone volume fraction [73]. Finally, it is possible to detect two-year longitudinal changes in bone microarchitectural parameters in subjects with OA, implying that disease progression can be monitored [74].

## 5 Conclusions

MRI provides a noninvasive means to detect and monitor pathologic alterations in cartilage and subchondral bone on the macrostructural, microstructural, and even biochemical level in subjects with osteoarthritis. The ability to detect these changes in vivo will allow new insight into the pathogenesis of osteoarthritis and permit early diagnosis of osteoarthritis in subjects who are at risk. This knowledge and capability should ultimately accelerate the discovery and testing of novel therapies to treat osteoarthritis, a disease which represents an enormous socioeconomic and health burden on society.

**Acknowledgments** This work was supported by research grants K23-AR059748, RO1-AR053133, R01-AR056260, and R01-AR060238 from the National Institute of Arthritis and Musculoskeletal and Skin Diseases (NIAMS), National Institutes of Health (NIH).

## References

1. Pleis, J.R., Lethbridge-Cejku, M.: Summary health statistics for U.S. adults: National Health Interview Survey, 2005. Vital and health statistics. Series 10, Data from the National Health Survey, 1 (2006)
2. Yelin, E., et al.: Medical care expenditures and earnings losses among persons with arthritis and other rheumatic conditions in 2003, and comparisons with 1997. *Arthritis Rheum.* **56**, 1397 (2007)
3. Burstein, D., Gray, M., Mosher, T., Dardzinski, B.: Measures of molecular composition and structure in osteoarthritis. *Radiol. Clin. North Am.* **47**, 675 (2009)
4. Wheaton, A.J., et al.: Proteoglycan loss in human knee cartilage: quantitation with sodium MR imaging – feasibility study. *Radiology* **231**, 900 (2004)

5. Burr, D.B.: Anatomy and physiology of the mineralized tissues: role in the pathogenesis of osteoarthritis. *Osteoarthritis Cartilage* **12**(Suppl A), S20 (2004)
6. Wehrli, F.W.: Structural and functional assessment of trabecular and cortical bone by micro magnetic resonance imaging. *J. Magn. Reson. Imaging* **25**, 390 (2007)
7. Felson, D.T., Neogi, T.: Osteoarthritis: is it a disease of cartilage or of bone? *Arthritis Rheum.* **50**, 341 (2004)
8. Resnick, D., Kang, H.S., Patterkieber, M.L.: *Internal Derangements of Joints*, 2nd edn. Saunders/Elsevier, Philadelphia (2006). pp. 2 v. (xvi, 2284, liv p.)
9. Eckstein, F., Burstein, D., Link, T.M.: Quantitative MRI of cartilage and bone: degenerative changes in osteoarthritis. *NMR Biomed.* **19**, 822 (2006)
10. Kamibayashi, L., Wyss, U.P., Cooke, T.D., Zee, B.: Trabecular microstructure in the medial condyle of the proximal tibia of patients with knee osteoarthritis. *Bone* **17**, 27 (1995)
11. Bobinac, D., Spanjol, J., Zoricic, S., Maric, I.: Changes in articular cartilage and subchondral bone histomorphometry in osteoarthritic knee joints in humans. *Bone* **32**, 284 (2003)
12. Layton, M.W., et al.: Examination of subchondral bone architecture in experimental osteoarthritis by microscopic computed axial tomography. *Arthritis Rheum.* **31**, 1400 (1988)
13. Chappard, C., et al.: Subchondral bone micro-architectural alterations in osteoarthritis: a synchrotron micro-computed tomography study. *Osteoarthritis Cartilage* **14**, 215 (2006)
14. Recht, M.P., Piraino, D.W., Paletta, G.A., Schils, J.P., Belhobek, G.H.: Accuracy of fat-suppressed three-dimensional spoiled gradient-echo FLASH MR imaging in the detection of patellofemoral articular cartilage abnormalities. *Radiology* **198**, 209 (1996)
15. Disler, D.G., McCauley, T.R., Wirth, C.R., Fuchs, M.D.: Detection of knee hyaline cartilage defects using fat-suppressed three-dimensional spoiled gradient-echo MR imaging: comparison with standard MR imaging and correlation with arthroscopy. *AJR Am. J. Roentgenol.* **165**, 377 (1995)
16. Potter, H.G., Linklater, J.M., Allen, A.A., Hannafin, J.A., Haas, S.B.: Magnetic resonance imaging of articular cartilage in the knee. An evaluation with use of fast-spin-echo imaging. *J. Bone Joint Surg. Am.* **80**, 1276 (1998)
17. Bredella, M.A., et al.: Accuracy of T2-weighted fast spin-echo MR imaging with fat saturation in detecting cartilage defects in the knee: comparison with arthroscopy in 130 patients. *AJR Am. J. Roentgenol.* **172**, 1073 (1999)
18. Peterfy, C.G., et al.: Whole-organ magnetic resonance imaging score (WORMS) of the knee in osteoarthritis. *Osteoarthritis Cartilage* **12**, 177 (2004)
19. Frobell, R.B.: Change in cartilage thickness, posttraumatic bone marrow lesions, and joint fluid volumes after acute ACL disruption: a two-year prospective MRI study of sixty-one subjects. *J. Bone Joint Surg. Am.* **93**, 1096 (2011)
20. Baranyay, F.J., et al.: Association of bone marrow lesions with knee structures and risk factors for bone marrow lesions in the knees of clinically healthy, community-based adults. *Semin. Arthritis Rheum.* **37**, 112 (2007)
21. Driban, J.B., et al.: Quantitative bone marrow lesion size in osteoarthritic knees correlates with cartilage damage and predicts longitudinal cartilage loss. *BMC Musculoskelet. Disord.* **12**, 217 (2011)
22. Wluka, A.E., et al.: Bone marrow lesions predict increase in knee cartilage defects and loss of cartilage volume in middle-aged women without knee pain over 2 years. *Ann. Rheum. Dis.* **68**, 850 (2009)
23. Hunter, D.J., et al.: Increase in bone marrow lesions associated with cartilage loss: a longitudinal magnetic resonance imaging study of knee osteoarthritis. *Arthritis Rheum.* **54**, 1529 (2006)
24. Torres, L., et al.: The relationship between specific tissue lesions and pain severity in persons with knee osteoarthritis. *Osteoarthritis Cartilage* **14**, 1033 (2006)
25. Zhang, Y., et al.: Fluctuation of knee pain and changes in bone marrow lesions, effusions, and synovitis on magnetic resonance imaging. *Arthritis Rheum.* **63**, 691 (2011)
26. Dardzinski, B.J., Mosher, T.J., Li, S., Van Slyke, M.A., Smith, M.B.: Spatial variation of T2 in human articular cartilage. *Radiology* **205**, 546 (1997)

27. Mosher, T.J., Dardzinski, B.J.: Cartilage MRI T2 relaxation time mapping: overview and applications. *Semin. Musculoskelet. Radiol.* **8**, 355 (2004)
28. Nieminen, M.T., et al.: T2 relaxation reveals spatial collagen architecture in articular cartilage: a comparative quantitative MRI and polarized light microscopic study. *Magn. Reson. Med.* **46**, 487 (2001)
29. Maroudas, A.I.: Balance between swelling pressure and collagen tension in normal and degenerate cartilage. *Nature* **260**, 808 (1976)
30. Venn, M., Maroudas, A.: Chemical composition and swelling of normal and osteoarthrotic femoral head cartilage. I. Chemical composition. *Ann. Rheum. Dis.* **36**, 121 (1977)
31. Maroudas, A., Venn, M.: Chemical composition and swelling of normal and osteoarthrotic femoral head cartilage. II. Swelling. *Ann. Rheum. Dis.* **36**, 399 (1977)
32. Mosher, T.J., Dardzinski, B.J., Smith, M.B.: Human articular cartilage: influence of aging and early symptomatic degeneration on the spatial variation of T2 – preliminary findings at 3 T. *Radiology* **214**, 259 (2000)
33. Li, X., et al.: In vivo T1(rho) and T(2) mapping of articular cartilage in osteoarthritis of the knee using 3 T MRI. *Osteoarthritis Cartilage* **15**, 789 (2007)
34. Peterfy, C.G., Schneider, E., Nevitt, M.: The osteoarthritis initiative: report on the design rationale for the magnetic resonance imaging protocol for the knee. *Osteoarthritis Cartilage* **16**, 1433 (2008)
35. Li, X., et al.: Spatial distribution and relationship of T1rho and T2 relaxation times in knee cartilage with osteoarthritis. *Magn. Reson. Med.* **61**, 1310 (2009)
36. Xia, Y., Moody, J.B., Alhadlaq, H.: Orientational dependence of T2 relaxation in articular cartilage: a microscopic MRI (microMRI) study. *Magn. Reson. Med.* **48**, 460 (2002)
37. Nishii, T., Kuroda, K., Matsuoka, Y., Sahara, T., Yoshikawa, H.: Change in knee cartilage T2 in response to mechanical loading. *J. Magn. Reson. Imaging* **28**, 175 (2008)
38. Shiomi, T., et al.: Loading and knee alignment have significant influence on cartilage MRI T2 in porcine knee joints. *Osteoarthritis Cartilage* **18**, 902 (2010)
39. Prasad, A.P., Nardo, L., Schooler, J., Joseph, G., Link, T.M.: T(1rho) and T(2) relaxation times predict progression of knee osteoarthritis. *Osteoarthritis Cartilage* **21**(1), 69–76 (2013)
40. Joseph, G.B., et al.: Baseline mean and heterogeneity of MR cartilage T2 are associated with morphologic degeneration of cartilage, meniscus, and bone marrow over 3 years – data from the osteoarthritis initiative. *Osteoarthritis Cartilage* **20**, 727 (2012)
41. Borthakur, A., et al.: Sodium and T1rho MRI for molecular and diagnostic imaging of articular cartilage. *NMR Biomed.* **19**, 781 (2006)
42. Regatte, R.R., Akella, S.V., Lonner, J.H., Kneeland, J.B., Reddy, R.: T1rho relaxation mapping in human osteoarthritis (OA) cartilage: comparison of T1rho with T2. *J. Magn. Reson. Imaging* **23**, 547 (2006)
43. Akella, S.V., et al.: Proteoglycan-induced changes in T1rho-relaxation of articular cartilage at 4T. *Magn. Reson. Med.* **46**, 419 (2001)
44. Menezes, N.M., Gray, M.L., Hartke, J.R., Burstein, D.: T2 and T1rho MRI in articular cartilage systems. *Magn. Reson. Med.* **51**, 503 (2004)
45. Keenan, K.E., et al.: Prediction of glycosaminoglycan content in human cartilage by age, T1rho and T2 MRI. *Osteoarthritis Cartilage* **19**, 171 (2011)
46. Witschey, W.R., et al.: T1rho MRI quantification of arthroscopically confirmed cartilage degeneration. *Magn. Reson. Med.* **63**, 1376 (2010)
47. Lattanzi, R., et al.: A B1-insensitive high resolution 2D T1 mapping pulse sequence for dGEMRIC of the HIP at 3 Tesla. *Magn. Reson. Med.* **66**, 348 (2011)
48. Siverson, C., et al.: Effects of B1 inhomogeneity correction for three-dimensional variable flip angle T1 measurements in hip dGEMRIC at 3 T and 1.5 T. *Magn. Reson. Med.* **67**, 1776 (2012)
49. Burstein, D., Gray, M.L., Hartman, A.L., Gipe, R., Foy, B.D.: Diffusion of small solutes in cartilage as measured by nuclear magnetic resonance (NMR) spectroscopy and imaging. *J. Orthop. Res.* **11**, 465 (1993)

50. Trattng, S., et al.: MRI visualization of proteoglycan depletion in articular cartilage via intravenous administration of Gd-DTPA. *Magn. Reson. Imaging* **17**, 577 (1999)
51. Kim, Y.J., Jaramillo, D., Millis, M.B., Gray, M.L., Burstein, D.: Assessment of early osteoarthritis in hip dysplasia with delayed gadolinium-enhanced magnetic resonance imaging of cartilage. *J. Bone Joint Surg. Am.* **85-A**, 1987 (2003)
52. Owman, H., Tiderius, C.J., Neuman, P., Nyquist, F., Dahlberg, L.E.: Association between findings on delayed gadolinium-enhanced magnetic resonance imaging of cartilage and future knee osteoarthritis. *Arthritis Rheum.* **58**, 1727 (2008)
53. Kim, S.D., Jessel, R., Zurakowski, D., Millis, M.B., Kim, Y.J.: Anterior delayed gadolinium-enhanced MRI of cartilage values predict joint failure after periacetabular osteotomy. *Clin. Orthop. Relat. Res.* **470**(12), 3332–3341 (2012)
54. Lattanzi, R., et al.: A new method to analyze dGEMRIC measurements in femoroacetabular impingement: preliminary validation against arthroscopic findings. *Osteoarthritis Cartilage* **20**, 1127 (2012)
55. Regatte, R.R., Schweitzer, M.E.: Novel contrast mechanisms at 3 Tesla and 7 Tesla. *Semin. Musculoskelet. Radiol.* **12**, 266 (2008)
56. Borthakur, A., et al.: Sensitivity of MRI to proteoglycan depletion in cartilage: comparison of sodium and proton MRI. *Osteoarthritis Cartilage* **8**, 288 (2000)
57. Shapiro, E.M., et al.: Sodium visibility and quantitation in intact bovine articular cartilage using high field (23)Na MRI and MRS. *J. Magn. Reson.* **142**, 24 (2000)
58. Wang, L., et al.: Rapid isotropic 3D-sodium MRI of the knee joint in vivo at 7T. *J. Magn. Reson. Imaging* **30**, 606 (2009)
59. Madelin, G., Lee, J.S., Inati, S., Jerschow, A., Regatte, R.R.: Sodium inversion recovery MRI of the knee joint in vivo at 7T. *J. Magn. Reson.* **207**, 42 (2010)
60. Chang, G., et al.: Improved assessment of cartilage repair tissue using fluid-suppressed (2)(3)Na inversion recovery MRI at 7 Tesla: preliminary results. *Eur. Radiol.* **22**, 1341 (2012)
61. Ling, W., Regatte, R.R., Navon, G., Jerschow, A.: Assessment of glycosaminoglycan concentration in vivo by chemical exchange-dependent saturation transfer (gagCEST). *Proc. Natl. Acad. Sci. U.S.A.* **105**, 2266 (2008)
62. Singh, A., et al.: Chemical exchange saturation transfer magnetic resonance imaging of human knee cartilage at 3 T and 7 T. *Magn. Reson. Med.* **68**, 588 (2012)
63. Lee, J.S., Regatte, R.R., Jerschow, A.: Isolating chemical exchange saturation transfer contrast from magnetization transfer asymmetry under two-frequency RF irradiation. *J. Magn. Reson.* **215**, 56 (2012)
64. Raya, J.G., et al.: Articular cartilage: in vivo diffusion-tensor imaging. *Radiology* **262**(2), 550–559 (2012)
65. Filidoro, L., et al.: High-resolution diffusion tensor imaging of human patellar cartilage: feasibility and preliminary findings. *Magn. Reson. Med.* **53**, 993 (2005)
66. Meder, R., de Visser, S.K., Bowden, J.C., Bostrom, T., Pope, J.M.: Diffusion tensor imaging of articular cartilage as a measure of tissue microstructure. *Osteoarthritis Cartilage* **14**, 875 (2006)
67. Deng, X., Farley, M., Nieminen, M.T., Gray, M., Burstein, D.: Diffusion tensor imaging of native and degenerated human articular cartilage. *Magn. Reson. Imaging* **25**, 168 (2007)
68. Banerjee, S., et al.: Rapid in vivo musculoskeletal MR with parallel imaging at 7T. *Magn. Reson. Med.* **59**, 655 (2008)
69. Saha, P.K., Wehrli, F.W., Gomberg, B.R.: Fuzzy distance transform: theory, algorithms, and applications. *Comput. Vis. Image Underst.* **86**, 171 (2002)
70. Saha, P.K., Gomberg, B.R., Wehrli, F.W.: Three-dimensional digital topological characterization of cancellous bone architecture. *Int. J. Imaging Syst. Technol.* **11**, 81 (2000)
71. Rajapakse, C.S., et al.: Computational biomechanics of the distal tibia from high-resolution MR and micro-CT images. *Bone* **47**, 556 (2010)
72. Lindsey, C.T., et al.: Magnetic resonance evaluation of the interrelationship between articular cartilage and trabecular bone of the osteoarthritic knee. *Osteoarthritis Cartilage* **12**, 86 (2004)

73. Bolbos, R.I., et al.: Relationship between trabecular bone structure and articular cartilage morphology and relaxation times in early OA of the knee joint using parallel MRI at 3 T. *Osteoarthritis Cartilage* **16**, 1150 (2008)
74. Blumenkrantz, G., et al.: A pilot, two-year longitudinal study of the interrelationship between trabecular bone and articular cartilage in the osteoarthritic knee. *Osteoarthritis Cartilage* **12**, 997 (2004)